Table 2

Renal Effects of DOCA

	GFR ml/Kg/Hr	Urine Flow ml/Kg/Hr	U_{osm} mOs/Kg H_2O	$U_{Na}V$ μEq/Kg/Hr	U_KV μEq/Kg/Hr	$U_{urea}V$ μM/Kg/Hr
Controls	1.9 ± 0.5	0.34 ± 0.08	760 ± 151	91 ± 32	25 ± 22	19 ± 13
DOCA	1.7 ± 0.8	0.46 ± 0.18	703 ± 112	120 ± 57	15 ± 8	23 ± 12

MEANS ± SEM

sodium and potassium balance in dogfish, then both role and major site of action contrast with those in mammals.

These studies were partially funded by NSF GB 35263, and by NIH AM 05077.

2 • 1975

The Length Tension Relation in the Single Cell Layered Myocardium of *Boltenia ovifera*

Lars Cleeman, Douglas L. Mayers, Yale Goldman, and Martin Morad. Department of Physiology, University of Pennsylvania School of Medicine

The heart of the tunicate ***Boltenia ovifera*** (the sea potato) consists of a straight tube which propels blood through a primitive circulatory system by means of a peristaltic contraction. In the MDIBL Bulletin of 1972, 1973. and 1974, and in SCIENCE (186: 750, 1974), we have reported on some of the contractile and electrical properties of this single cell layered myocardium. In the present report, we have attempted to investigate the length-tension characteristics of this myocardium under conditions where length of the preparation was clamped to various values.

The sea potato heart was removed from the animal and was cannulated at one end. The pericardium was dissected away and an incision was made along the longitundinal raphe of the heart. This procedure produces a single cell layered sheet of muscular tissue. The sheet was placed over the opening of a lucite chamber separating the solution on the luminal side of the preparation electrically and mechanically from the solution of the extraluminal side. A silicone paste was applied around the edges of the opening to electrically seal the injured areas of the myocardium. The longitudinal ends of the myocardial preparation were snared down with nylon strings into two grooves running close to the opening covered with the tissue. The short ends of the preparation were then pressed down with two silastic wedges mounted on two micro-manipulators. With the preparation in place, Evans blue dye was injected into the bottom compartment of the chamber to check for leaks around the edges and the mechanical continuity of the preparation. The lower chamber pressure was slightly increased as to produce a gentle "bulge" in the myocardial preparation (see Figure 1 B). The height of the bulge could be observed on a calibrated grid in the dissection microscope. A light beam passing through the upper chamber (Figure 1 A) and focused in a vertical slit on the muscle was used to give an automatic measurement of the bulge height. The blue dye injected into the lower chamber was essential to increase the light blocking capabilities of the bulge as the tissue is highly transparent. The light source was an array of 9 light emitting diodes. The light source was chopped electrically at 40 KHz frequency. A phase lock amplifier was used to increase the signal to noise ratio of the measured transmitted light.

Increasing the height of the bulge decreases transmitted light. The pressure difference across the tissue was measured with a Statham pressure strain guage connected to the closed lower chamber (the surface of the fluid in the open upper chamber was held at a constant level). Eliciting a contraction by transepithelial electrical stimulation the height of the bulge decreases, thus increasing the transmitted light. The time course of transmission of light is directly related to the time course of the shortening of the myocardial preparation. The lower trace and the upper trace of Figure 2 A show the time course of pressure and transmitted light. Consistent with our previous observation we found that only depolarization of the luminal membrane produces contraction. The transepithelial resistance range between 75-200 Ω cm^2. Unlike the preparation used in the previous years, the sheet preparation did not show the graded contractile response with increasing stimulus strength.

In order to maintain a constant length during the time course of contraction, servo-control was applied to keep the bulge height constant. The light signal measured with the photodiode was compared with an adjustable reference and the difference was amplified and fed to a servo-controlled motor (Gould Brush, Mark 220) converting the electrical signal to an angular position. A crank shaft attached to the axis of the motor was hinged to a rod in rigid connection with a piston which displaced sufficient fluid to clamp the height of the bulge. The DC loop gain of the system was approximately 10. Effective clamp control of the height of the bulge could often be obtained within 25 msec. Figure 2 A shows the time course of contraction and the light signal with the loop open (top and bottom traces), and with the loop closed (middle two traces). Note that the light signal hardly changes when the loop is closed and that the pressure signal is strongly enhanced.

Figure 2 B shows the isometric pressure records from the bulge-clamped preparation where the bulge height is changed stepwise between individual recordings. As the height of the bulge and thereby the length of the preparation is decreased, the maximum twitch pressure decreases. A resting pressure is only observed for the first three records where the muscle was stretched considerably. Laplaces law was applied to derive the wall tension, T, from the pressure, P, and the radius of bulge curvature, r. The bulge was assumed to approximate a segment of a circular cylinder. Very little curvature is observed in the central region when the bulge is observed from the side (see Figure 1 B). The radius of the cylinder was estimated according to the schematic shown in Figure 1 C, also showing the relation between the bulge height and the length of the preparation, 1.

In Figure 1 B, the twitch pressure obtained with maximal bulge height (h = 1.2 mm) is P = 1.5 cm H_2O = 1.5 g/cm^2. The radius of the bulge is r = $(1.2^2 + 1.125^2) / (2 \cdot 1.2)$mm =

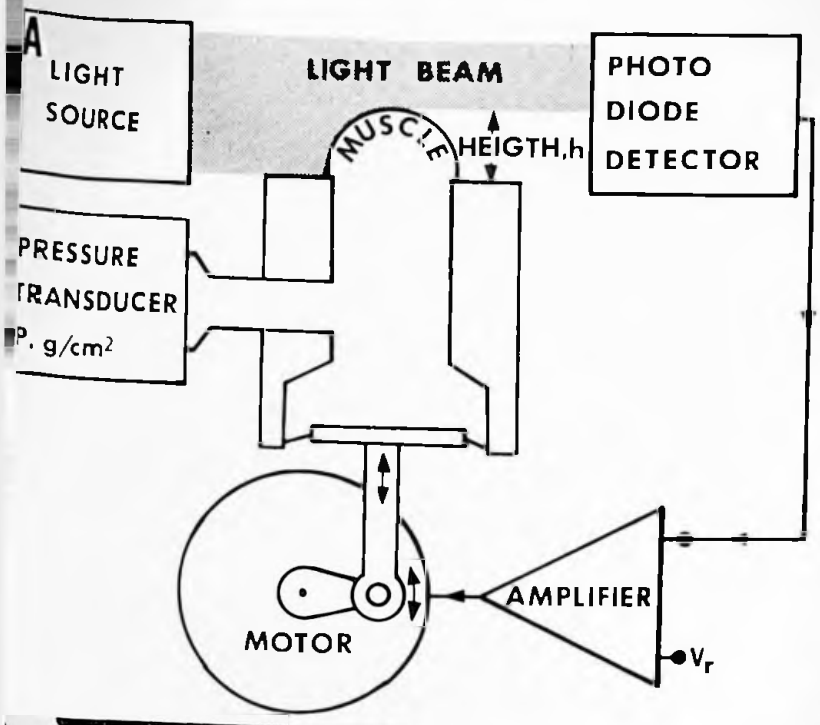

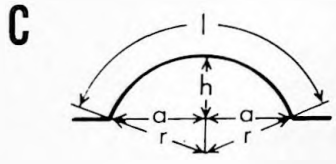

$r=(h^2+a^2)/(2\cdot h)$

$l=2\cdot r\cdot \mathrm{Arctan}(a/(r-h))$

Figure 1 Panel A shows a simplified diagram of the bulge-clamp apparatus. The light beam emitted from the light source is partially blocked by the bulge of muscular tissue. The transmitted light indicating the height of the bulge, h, is sensed with a photodiode detector; the signal is compared to a reference value V_r, and the amplified error signal drives a motor causing a volume displacement in the closed chamber under the bulge. Pressure changes are sensed with a transducer.
Panel B: the bulge photographed through the dissection microscope is observed in approximately the same direction as seen by the light beam. The light beam intersects the muscle in the central region where the arrow indicates the height of the bulge, $h \cong 1$ mm.
Panel C: the dimensions of the circular arch describing the cross section of the bulge is determined by the measured height, h, and the width, $2 \cdot a = 2.25$ mm. The radius of curvature, r, and the length of the tissue, l, are calculated from height and weight using the indicated equations.

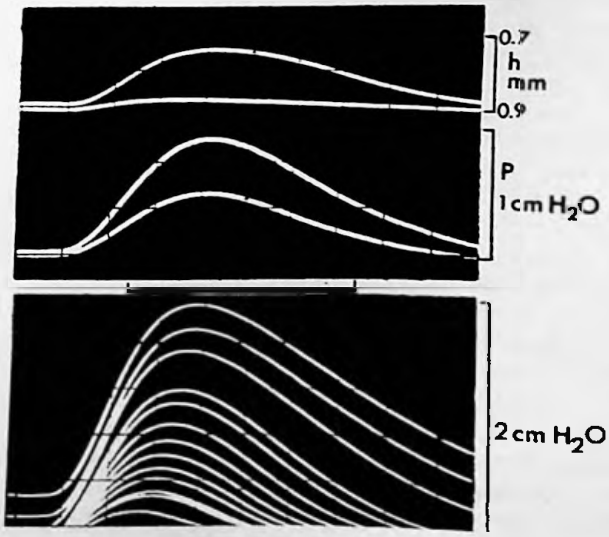

Figure 2 The two upper traces in panel A are recordings of the bulge height during a twitch and the two lower traces are recordings of twitch pressure. With the feed back loop closed, the height of the bulge remains nearly constant (0.9 mm) during the twitch and twitch pressure is greatly increased (75/08/25). In panel B the twitch pressure from the bulge-clamped preparation is recorded for different values of the bulge height. The bulge height is decreased stepwise from 1.2 to 0.9 mm (75/08/28).

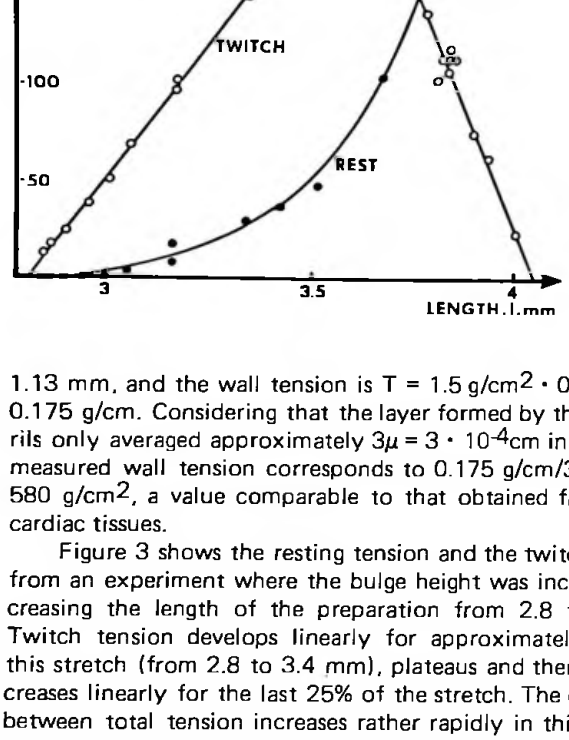

Figure 3 The twitch tension and the resting tension are plotted versus the lenth of the preparation. Length and radius of curvature are calculated from the height of the bulge using the equations in Fig. 1, panel C. The wall tension is calculated as the product of the pressure and the radius of curvature, preparation from (75/08/21).

1.13 mm, and the wall tension is T = 1.5 g/cm^2 · 0.113 cm = 0.175 g/cm. Considering that the layer formed by the myofibrils only averaged approximately 3μ = 3 · 10^{-4}cm in width the measured wall tension corresponds to 0.175 g/cm/3 · 10^{-4} = 580 g/cm^2, a value comparable to that obtained from other cardiac tissues.

Figure 3 shows the resting tension and the twitch tension from an experiment where the bulge height was increased, increasing the length of the preparation from 2.8 to 4 mm. Twitch tension develops linearly for approximately 50% of this stretch (from 2.8 to 3.4 mm), plateaus and thereafter decreases linearly for the last 25% of the stretch. The difference between total tension increases rather rapidly in this last segment of the stretch. The difference between total tension and twitch tension is plotted as resting tension in Figure 3. Longer stretches beyong the maximum twitch tension often produce irreversible damage to the single cell layered myocardium. Such stretches lowered the active length-tension curve markedly without altering the passive length tension curve.

The examination of the time course of the developed tension at various muscle lengths consistently showed a prolongation of the time to peak tension with increasing length. The rate of rise also seems to increase with increasing tension. This later observation suggests that stretch increases activation of the myocardium.

The shape of the length-tension curve is quite similar to the length tension curve obtained from a single fiber of frog skeletal muscle (Gordon, Juxley and Julian, J. Physiol. 184, p. 174, 1966). However, since in the present experiment sarcomere length was not measured further analogy with the skeletal muscle observations could be misleading. It is of interest to note that the region of the length-tension curve where active tension is observed (ca. 0.8 lmax to ca. 1.5 lmax) is only a small fraction of that observed in vertebrate skeletal muscle (ca. 0.6 lmax to 1.7 lmax).

Comparison of the length-tension curves obtained in these experiments with those obtained from mammalian ventricular muscle show a marked similarity in the onset and magnitude of the resting tension. In contrast to the linear ascending limb of the length-tension curve obtained with this preparation, the vertebrate myocardial preparations show considerable curvature. This curvature has been explained on basis of the structural complexity (more than one cell layer and fiber branching) of vertebrate cardiac muscle (Julian, Michael and Solin Circ. Res. 37, p. 299, 1975; and Pollack and Huntsman, Am. Physiol. 227, p. 383, 1974).

Although present results seem to be qualitatively simi to those of vertebrate skeletal muscle, the measurements sarcomere length is mandatory for determination of filame overlap for such a comparison. We hope to measure the sarc mere length in this preparation by combining laser diffrac tic technique with our present system.

Supported by HL 16152 and HL 17702.

3 • 1975

Control of Polar Lobe Formation and Connective Tissu Biosynthesis in Embryos of *Ilyanassa obsoleta*

Gary W. Conrad and Gail L. Pakstis; Division of Biolog Kansas State University

Fertilized eggs of the marine neogastopod mudsnail, ***Ily anassa obsoleta***, form and resorb a series of cytoplasmic protu berances from the vegetal pole of the cell before and durin first cleavage. These protuberances, called polar lobes, appea to form by constriction of a band of microfilaments in the co tical cytoplasm of the spherical zygote cell (J. Cell Biol., 5 228-233, 1973). The factors normally controlling this lobin activity are not known. If polar lobes are removed surgically the time of first cleavage, the resultant "lobeless" embryos d velop during the following week into veliger larvae which, histological criteria, lack several tissues, e.g., external she foot, operculum, heart, intestine, eyes, and statocysts. O property shared by the missing tissues is the synthesis of lar amounts of extracellular macromolecules. The purpose of o research has been to 1) elucidate factors controlling polar lob formation, and 2) determine the degree to which morphoge etic factors in the polar lobe cytoplasm of the fertilized e subsequently affect synthesis and polymerization of extrace ular matrices.

Ilyanassa obsoleta (Nassarius obsoletus) was collected the northeast side of Thompson Island and kept in running s